Science Advances

AAAS

advances.sciencemag.org/cgi/content/full/2/7/e1600274/DC1

Supplementary Materials for

Liquid biopsy and therapeutic response: Circulating tumor cell cultures for evaluation of anticancer treatment

Bee Luan Khoo, Gianluca Grenci, Tengyang Jing, Ying Bena Lim, Soo Chin Lee, Jean Paul Thiery, Jongyoon Han, Chwee Teck Lim

Published 13 July 2016, *Sci. Adv.* **2**, e1600274 (2016)
DOI: 10.1126/sciadv.1600274

The PDF file includes:

- table S2. Samples for preliminary validation of procedure.
- table S3. Samples evaluated for drug screening.
- table S4. Average percentage of viable $CD45^-$ cells in clinical samples.
- table S5. Disease evaluation of three sets of serial samples with at least one positive culture generated.
- table S6. CTC counts per milliliter as reported by notable CTC enrichment methods (non–culture-based).
- Legend for movie S1

Other Supplementary Material for this manuscript includes the following:
(available at advances.sciencemag.org/cgi/content/full/2/7/e1600274/DC1)

- movie S1 (.mp4 format). Illustration of seeding, growth, and drug flow.

Supplementary Figures

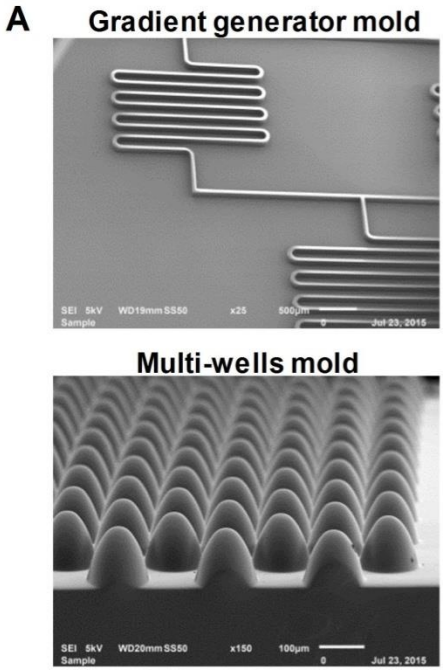

fig. S1. Microfabricated molds for the assay.

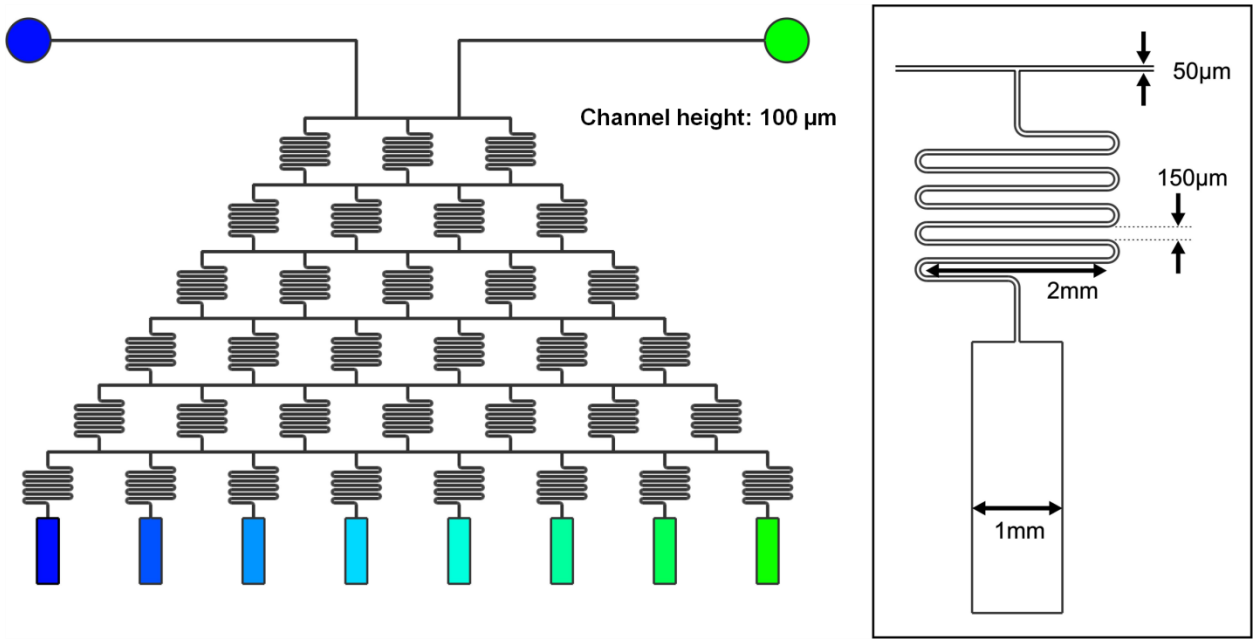

fig. S2. Schematics of the gradient generator design.

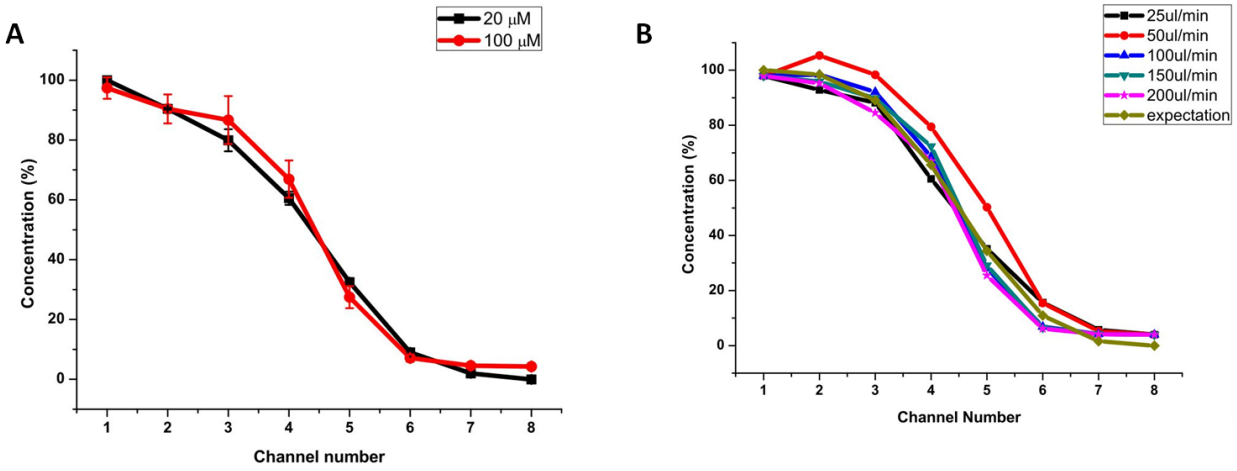

fig. S3. Flow rate of the device and the dynamics within the channel. (**A**) Relative fluorescein isothiocyanate (FITC) dye concentration measured in 8 cell culture channels using different initial dye concentrations. The resulting dye concentrations across the channels were consistent between two different input conditions. (**B**) Relative FITC dye concentration measured in 8 cell culture channels under different flow rates. As observed from the calibration results, the lower flow rates had a gentler gradient as compared to the higher flow rates. This can be explained by the longer duration that the reagent stayed within the device, eventually enabling more time for diffusion across channels. The steeper gradient at higher flow rates could be caused by inefficient mixing of the liquid in the serpentine due to the shorter transit duration. Although the device performed robustly under various flow rates, we decided to run the subsequent experiments at 100 µl/min as the flow profile generated was closest to that calculated.

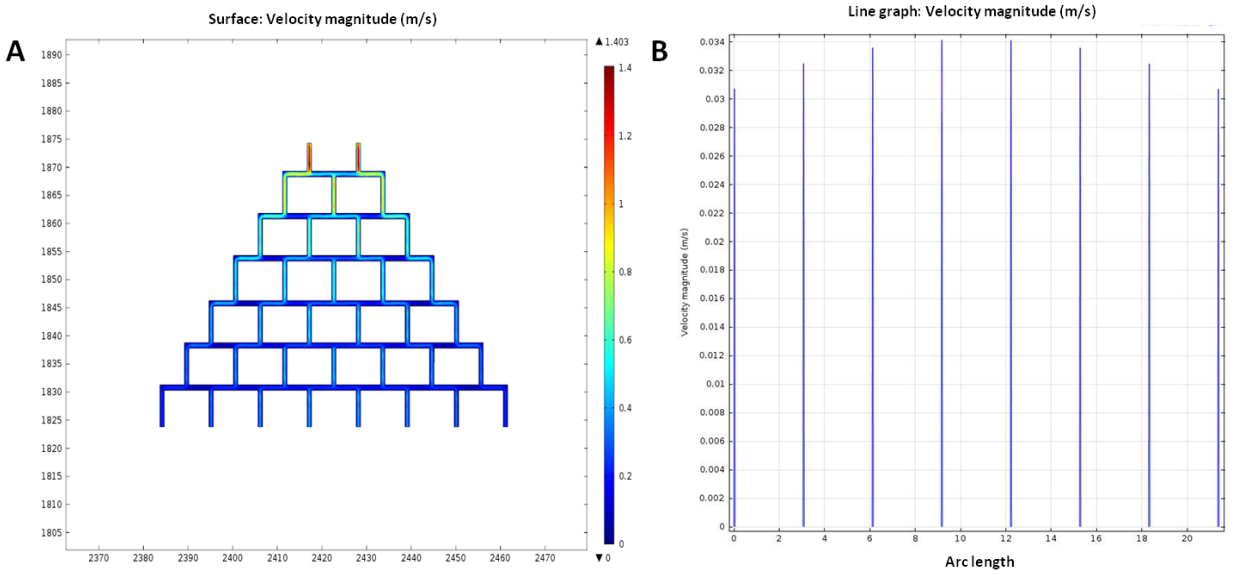

fig. S4. Simulated flow conditions of the assay. (**A**) Simulated flow condition in a simplified gradient generator design using COMSOL. The flow rate was colored coded as shown in the right legend. (**B**) Simulated flow rate at the eight individual outlets using COMSOL. The flow rate of the centre outlet was about 0.034m/s while the flow rate of the side outlet was about 0.031m/s.

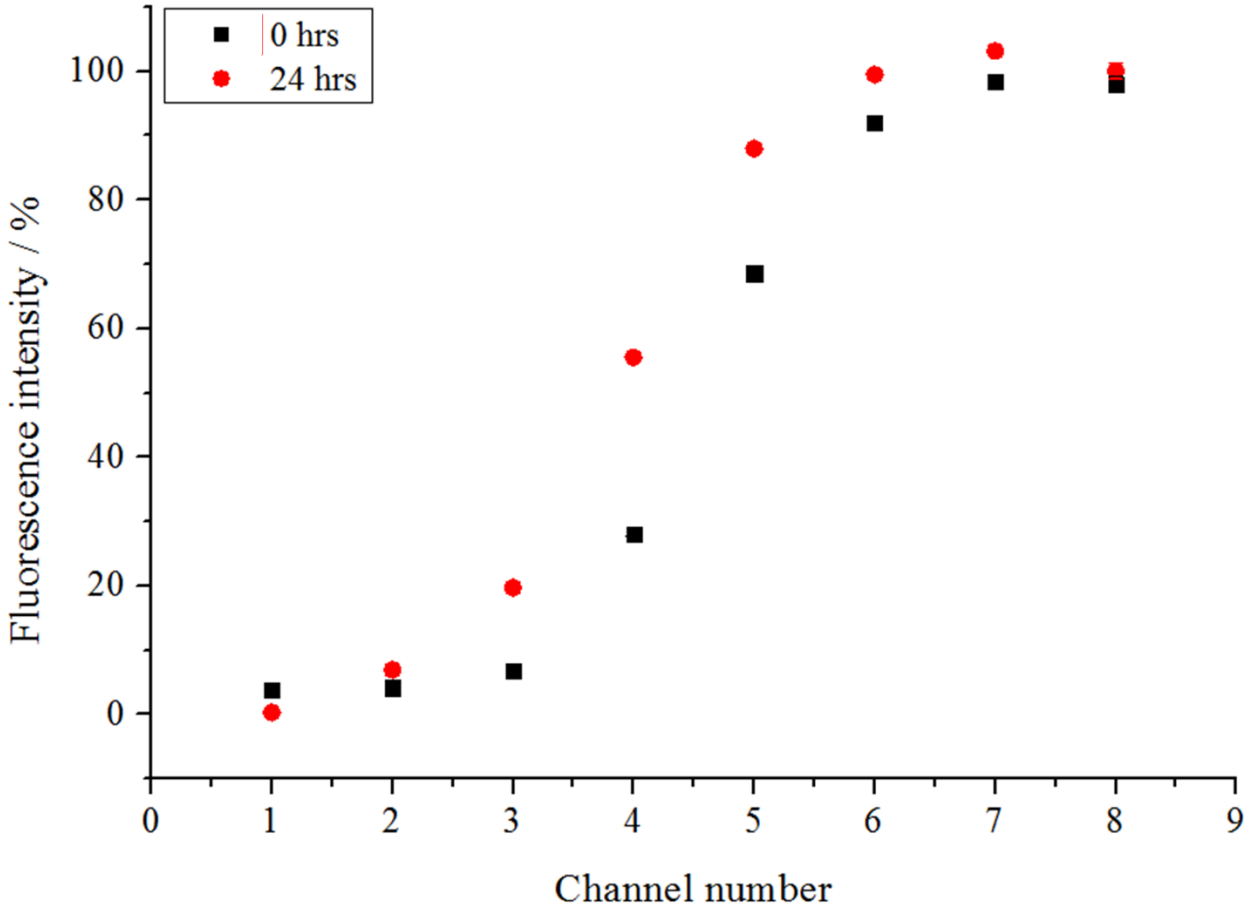

fig. S5. Consistency of gradient concentration in channels over time. After generation of gradient via inward flow of 100% dye and deionized (Di) water (T= 0 hrs), the assay was incubated under dark conditions. Channel contents were sampled at T = 0 and 24 hrs. Scatter plot shows that the concentrations in each channel remains relatively constant over time ($p<0.05$).

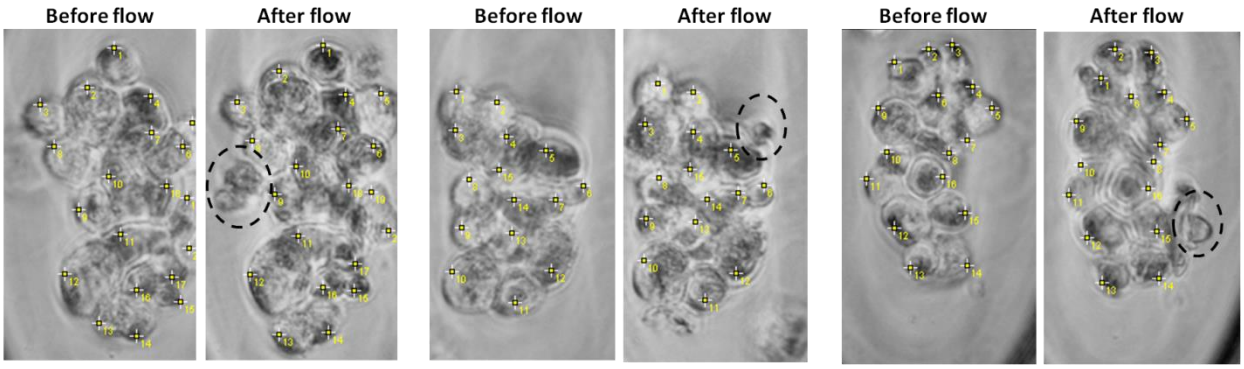

fig. S6. Estimation of cell counts after influence of flow. Arrangement of cells within a cluster was retained, and can be enumerated to determine cell loss. Some smaller cells might detach from the microwells within the upper channel and drift to microwells within the middle or lower channel regions.

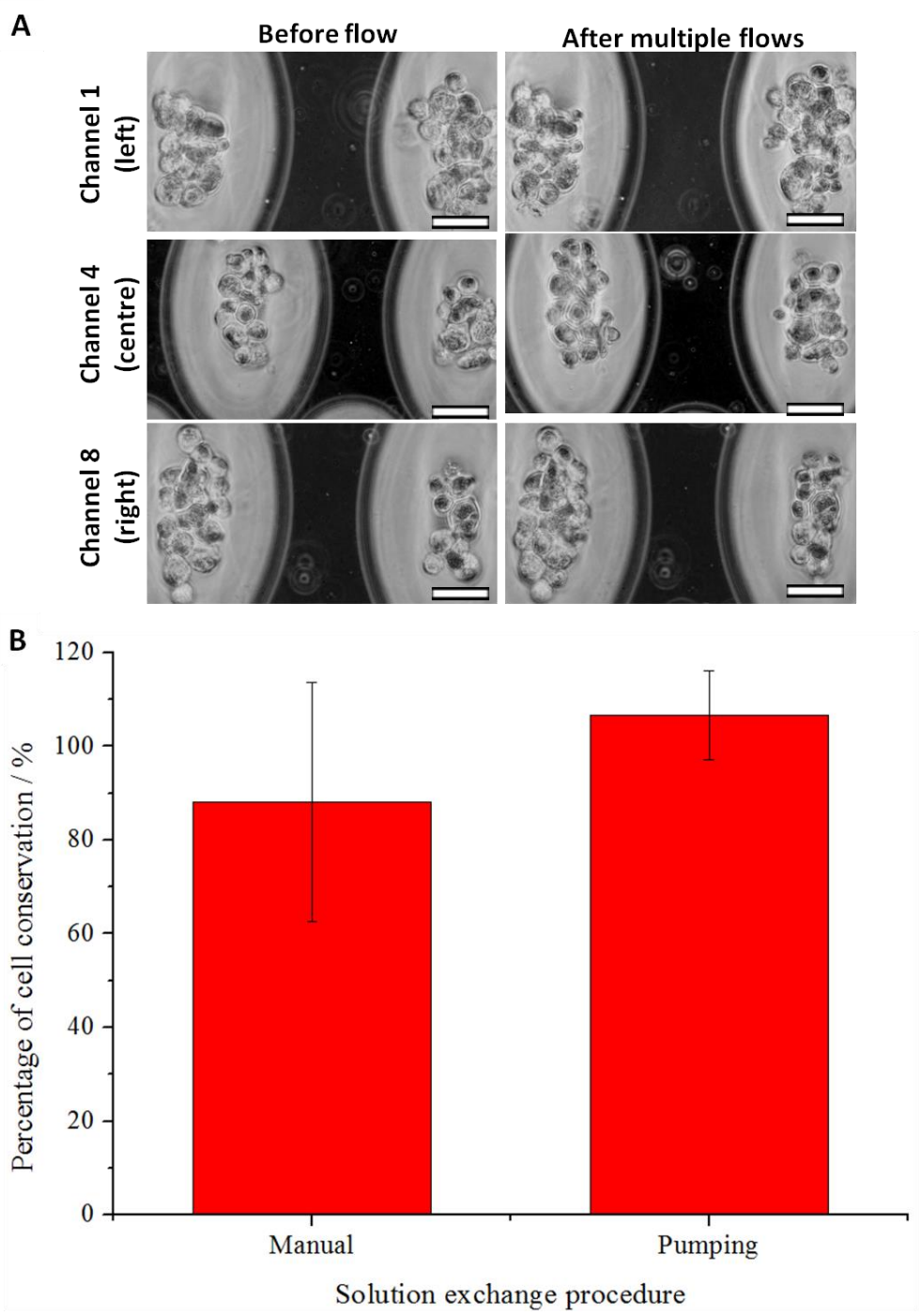

fig. S7. Validation of integrated assay for proliferation with MCF-7 cell lines. (**A**) Representative images of enclosed cells in microwells before and after multiple pumping of inward and outward flow sets at 100 µl/min using syringe pumps. Cluster morphology was retained under flow. Scale bar is 50 µm. (**B**) Comparison of percentage of cell conservation (number of cells in each microwell) before and after solution exchange. Two methods were tested, namely manual pipetting (manual) and using syringe pumps (pumping). Bar graphs illustrates that the changes in cell count within microwells were significant under the effects of pumping ($p = 0.203715$).

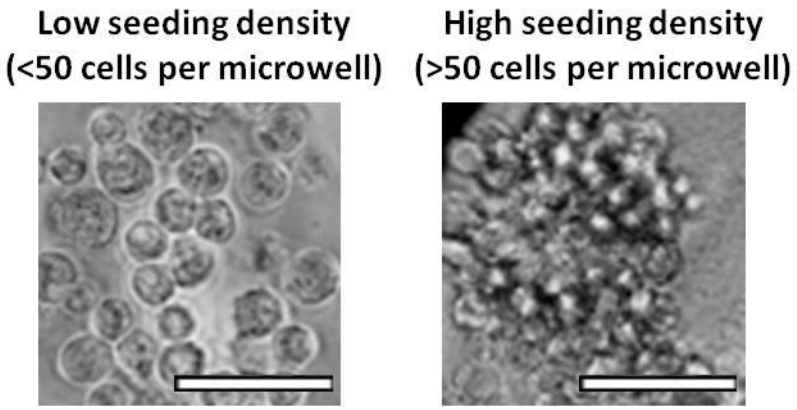

fig. S8. Optimization of cancer cell line culture parameters. Phase contrast images of cancer cell line cultures in microwell-based assay. Low seeding density did not generate cluster formation. Scale bar is 50 μm.

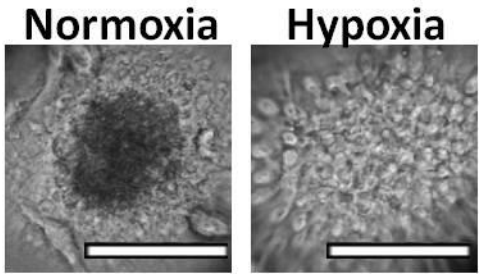

fig. S9. Phase-contrast images of 2-week cultures under different culture conditions. Multilayered clusters were only formed in the presence of microwells under hypoxia. In microwells under normoxia, only a loose monolayer of cells (possibly blood cells) was found. Scale bar is 50 μm.

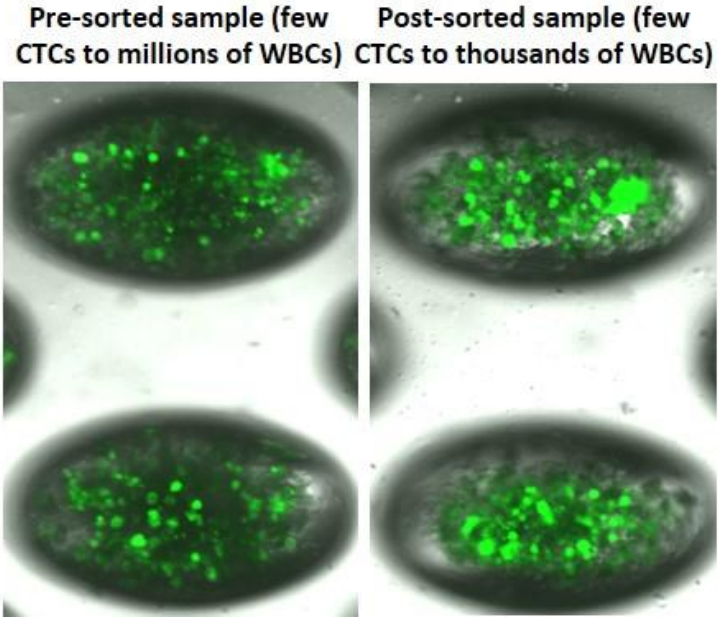

fig. S10. Proportion of CTCs before culture affected the potential of cluster formation. Samples which did not generate clusters after culture (left) might be able to demonstrate cluster formation after CTCs were enriched and reseeded back to a smaller fraction of patient nucleated blood cells (right).

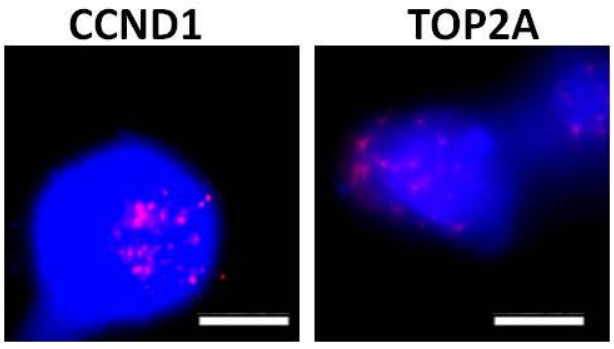

fig. S11. Fluorescence in situ hybridization of cultured cells. Representative images of cancer cells with heightened expression of cancer associated genes, namely CCND1 and TOP2A. Scale bar is 5 μm.

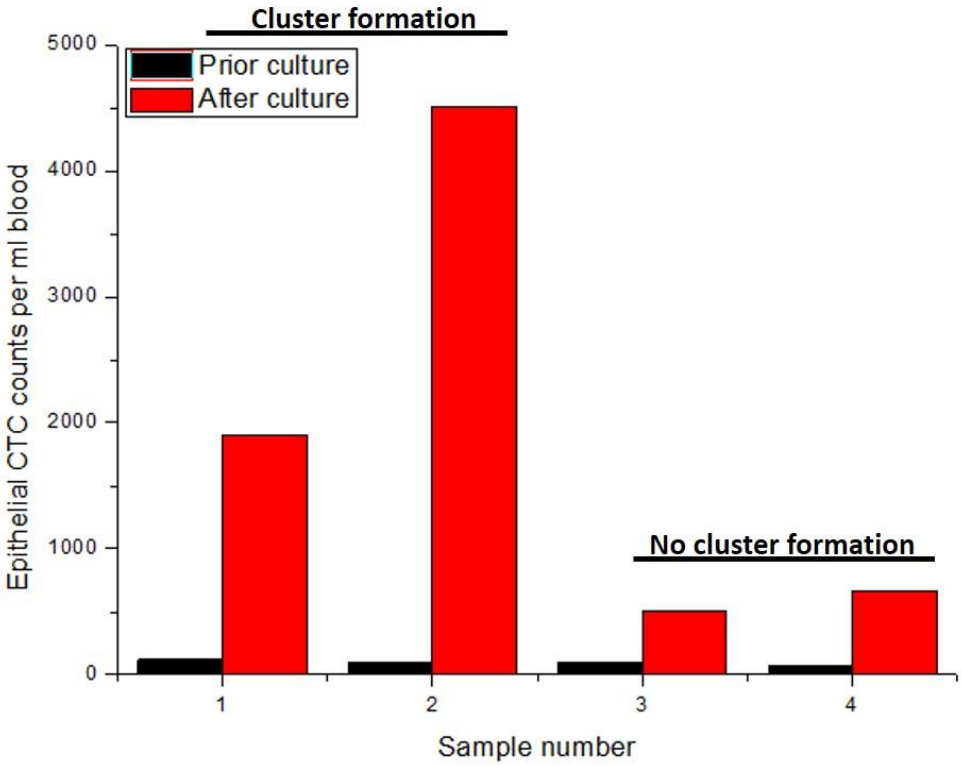

fig. S12. Epithelial CTC counts before and after culture. Epithelial CTC counts appeared to correlate with cluster forming potential.

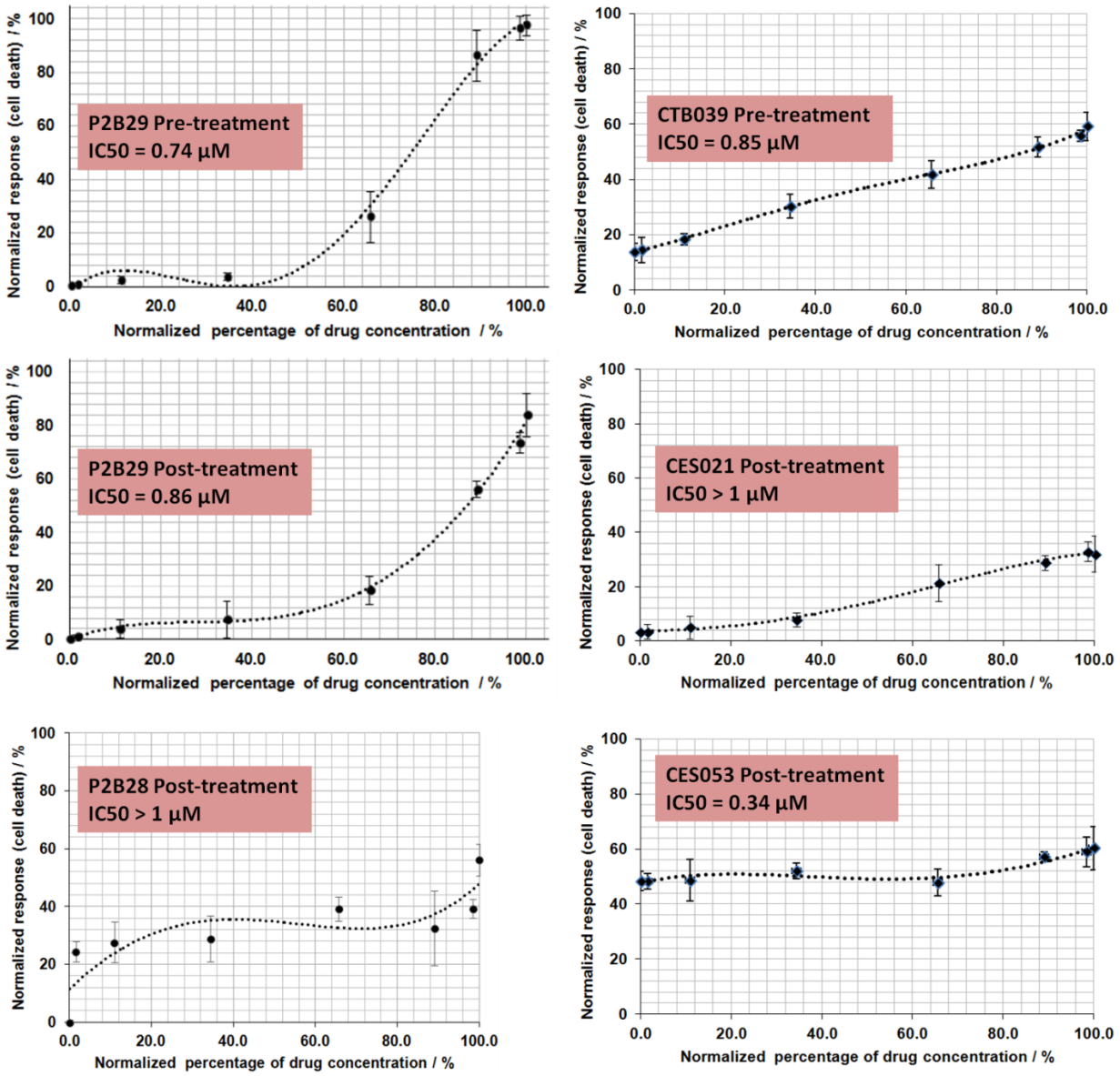

fig. S13. Screening of doxorubicin in microwell assay using clinical human primary cancer cells cultured from blood samples. Dose response curve and corresponding IC_{50} values generated from viability result of each sample. All error bars represented standard deviation (SD) of counts from 30 microwells of the same cultured samples.

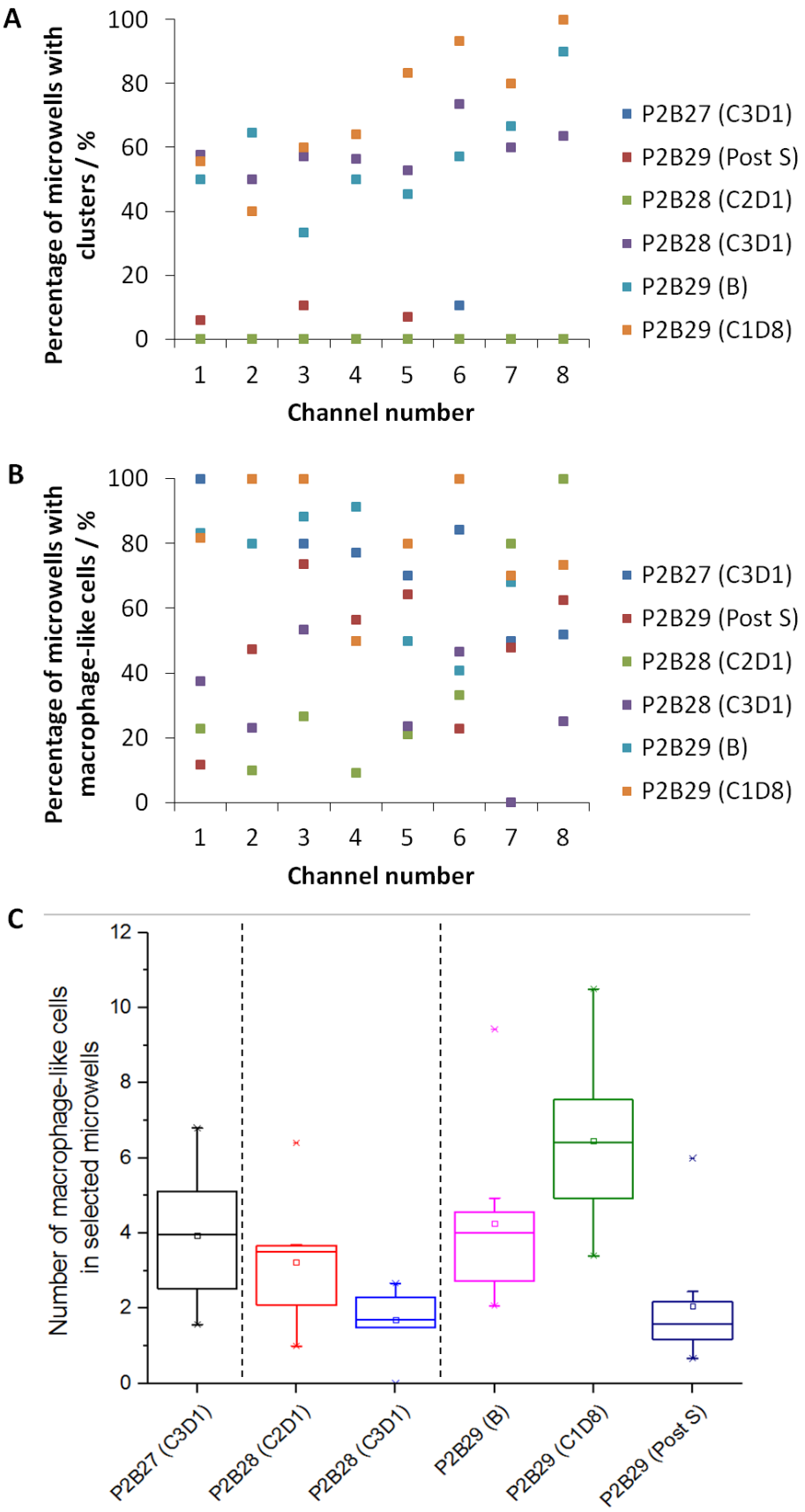

fig. S14. Characterization of cultures. (**A**) Percentage of microwells with clusters. (**B**) Percentage of microwells with macrophage-like cells. (**C**) Enumeration of macrophage-like cell count per microwell. Microwells without macrophage-like cells were not selected for count. S: Surgery; B: Baseline

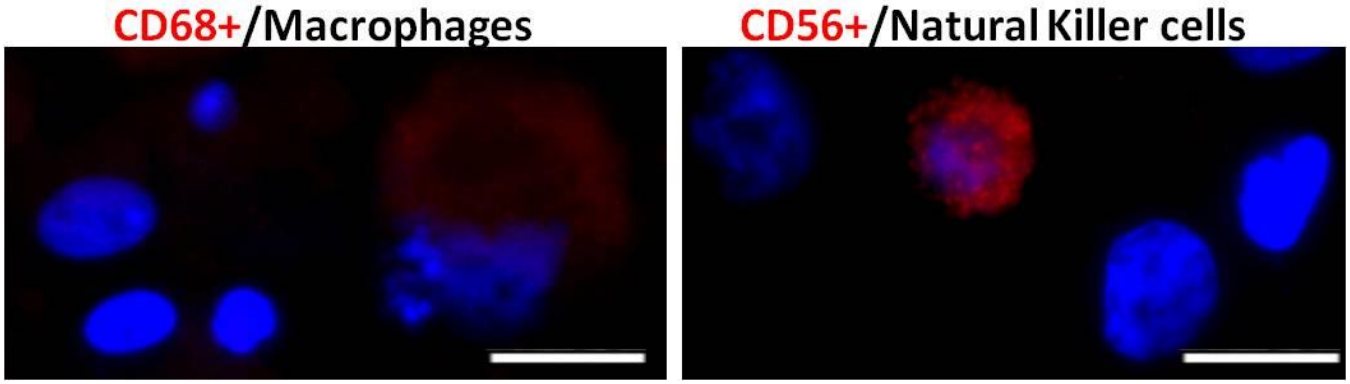

fig. S15. Representative images of residual WBC populations. Most leukocytes cannot be maintained as viable cells beyond a week in culture under hypoxic conditions, with the exception of specific populations. Blood cells of other lineages such as megakaryocytes and endothelial cells, as well as mesenchymal stem cells and their associated lineage cells were rarely detected (*1*). . Scale bar is 20 μm**.**

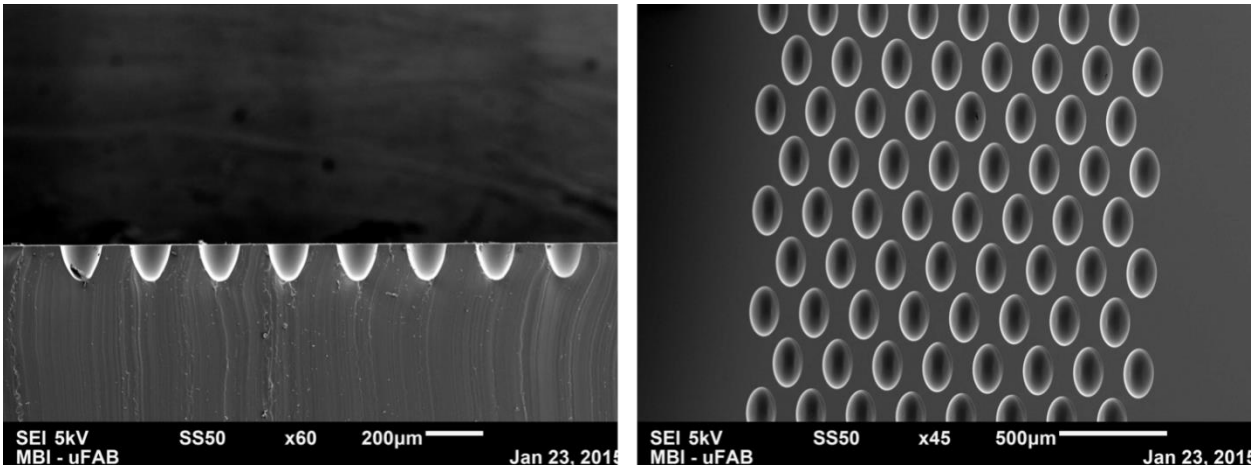

fig. S16. Scanning electron microscopy images demonstrating the densely packed array of microwells to maximize surface for capturing CTCs for culture. Cross-sectional image of microwells (Left). Overview of the microwell array (Right).

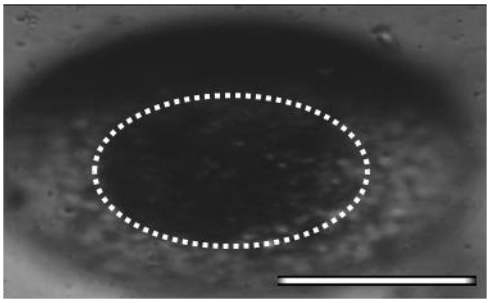

fig. S17. Representative image of a microwell containing cells contaminated by RBCs due to inadequate RBC lysis. Region of the RBC contamination is marked with a white dotted line. Scale bar is 100 μm.

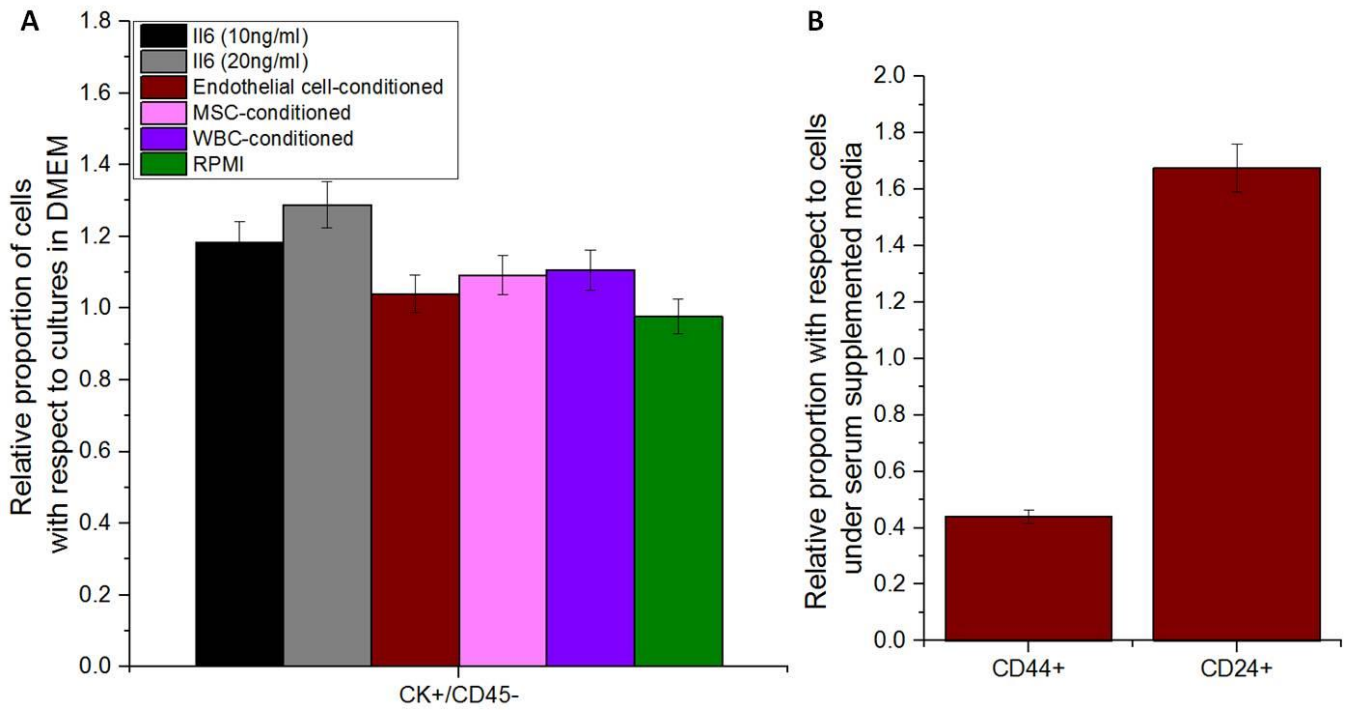

fig. S18. Optimization of culture media conditions. (**A**) Portions of each clinical sample were maintained separately with RPMI or under exposure to tumor promoting cytokine IL-6, as well as endothelial cell-, mesenchymal cell- and WBC- conditioned media. Characterization of the relative epithelial CK+ CTC population after culture suggests no significant variation (P value is 0.25) as compared to the epithelial CTC counts of cultures maintained under DMEM. (**B**) Proportion of breast cancer stem cells (CD44+/CD24-) were higher in samples maintained under serum-supplemented DMEM as compared to serum-free DMEM. Hence supplemented DMEM was selected for subsequent culture.

Supplementary Tables

table S1. Concentration of a single reagent at each serpentine. To calculate the concentration of the liquid at each serpentine, the concentration was averaged from the preceding serpentine outputs. For a single reagent, the concentration in channel 1 is the highest and that in channel 8 is the lowest.

	Channel number							
	1	**2**	**3**	**4**	**5**	**6**	**7**	**8**
Percentage of reagent / %	100.0	0.0						
	100.0	50.0	0.0					
	100.0	75.0	25.0	0.0				
	100.0	87.5	50.0	12.5	0.0			
	100.0	93.8	68.8	31.3	6.3	0.0		
	100.0	96.9	81.3	50.0	18.8	3.1	0.0	
	100.0	98.4	89.1	65.6	34.4	10.9	1.6	0.0

table S2. Samples for preliminary validation of procedure. Samples that did not form multilayered clusters were indicated as N, whereas those that formed multilayered clusters were labeled as Y. CTB: refractory metastatic disease cohort; CES: early-stage disease cohort; P2A/B: newly diagnosed disease cohort; and CRM: early-stage disease with no measurable tumor cohort.

Sample	ID	Time-point	Cluster
1	CTB 010	Post treatment	N
2	CTB 011	Post treatment	N
3	CTB 013	Post treatment	N
4	CTB 015	Pre-treatment	N
5	CTB 016	Pre-treatment	N
6	CTB 017	Pre-treatment	N
7	CTB035	Pre-treatment	Y
8	CES017	Post treatment	N
9	CES029	Post treatment	N
10	CES040	Post treatment	N
11	CES041	Pre-treatment	Y
12	CES041	Post treatment	Y
13	CES041	Post treatment	N
14	CES043	Post treatment	Y
15	CES045	Post treatment	N
16	CES045	Post treatment	N
17	CES049	Pre-treatment	Y
18	CES049	Post treatment	N
19	CES049	Post treatment	Y
20	CES057	Pre-treatment	N
21	CES057	Post treatment	N
22	CES060	Pre-treatment	N
23	CES060	Pre-treatment	Y

24	CES064	Pre-treatment	Y
25	CES67	Pre-treatment	N
26	CES68	Pre-treatment	Y
27	CES69	Pre-treatment	Y
28	CES70	Pre-treatment	N
29	P2A17	Post treatment	N
30	P2A21	Post treatment	N
31	P2A23	Post treatment	N
32	P2A27	Post treatment	N
33	P2A28	Pre-treatment	Y
34	P2A32	Post treatment	N
35	P2A33	Post treatment	N
36	P2A36	Pre-treatment	Y
37	P2B29	Post treatment	N
38	P2B30	Pre-treatment	Y
39	CRM001	Pre-treatment	Y
40	CRM003	Pre-treatment	Y
41	CRM007	Pre-treatment	Y
42	CRM007	Post treatment	Y
43	CRM011	Post treatment	Y
44	CRM013	Pre-treatment	N
45	CRM013	Post treatment	N
46	CRM044	Pre-treatment	Y
47	CRM048	Post treatment	N
48	CRM049	Post treatment	N
49	CRM051	Post treatment	N

table S3. Samples evaluated for drug screening. Samples that did not form multilayered clusters were indicated as N, whereas those that formed multilayered clusters were labeled as Y. CTB: refractory metastatic disease cohort; CES: early-stage disease cohort; P2A/B: newly diagnosed disease.

Sample	ID	Time-point	Cluster
1	CTB033	Post treatment	N
2	CTB038	Pre-treatment	N
3	CTB039	Pre-treatment	Y
4	CTB039	Post treatment	N
5	CES21	Post treatment	Y
6	CES033	Post treatment	N
7	CES036	Post treatment	N
8	CES039	Post treatment	N
9	CES045	Post treatment	N
10	CES050	Post treatment	N
11	CES050	Post treatment	N
12	CES052	Post treatment	N
13	CES053	Post treatment	Y
14	CES053	Post treatment	N
15	P2B27	Post treatment	N
16	P2B28	Pre-treatment	N
17	P2B28	Post treatment	N
18	P2B28	Post treatment	Y
19	P2B29	Pre-treatment	Y
20	P2B29	Post treatment	Y
21	P2A22	Post treatment	N
22	P2B17	Pre-treatment	N
23	P2B21	Post treatment	N
24	P2B21	Post treatment	N

table S4. Average percentage of viable CD45⁻ cells in clinical samples.

Percentage of drug (1 μM) / %	Percentage of viable CD45⁻ cells / %					
	P2B29 Pre-treatment	P2B29 Post-treatment	P2B28 Post-treatment	CTB039 Pre-treatment	CES21 Post-treatment	CES053 Post-treatment
100.0	0.4	0.4	0.0	40.8	67.9	39.8
98.4	0.7	1.1	24.4	44.2	66.9	41.0
89.1	2.6	4.1	27.6	48.3	71.1	42.8
65.6	3.9	7.7	28.8	58.3	78.6	52.2
34.4	26.2	18.5	39.2	69.7	92.0	48.0
10.9	86.4	56.2	32.6	81.6	94.9	51.4
1.6	96.6	73.6	39.3	85.5	96.4	51.7
0.0	97.8	84.0	56.2	86.2	96.7	51.7

table S5. Disease evaluation of three sets of serial samples with at least one positive culture generated. For P2B samples, first response result refers to clinical response after four cycles of pre-operative chemotherapy; second response result refers to response at surgery. pCR = pathological complete response.

ID	Time-point	Cluster	Tumor response	Patient survival
CTB039	Pre-treatment	Y		
CTB039	Post treatment	N	Partial response	Alive
P2B28	Pre-treatment	N		
P2B28	Post treatment	N		
P2B28	Post treatment	Y	56% reduction / no pCR	28/04/2016 (Alive)
P2B29	Pre-treatment	Y		
P2B29	Post treatment	Y	Completed 3 cycles of AC with clinical response / no pCR	20/05/2016 (Alive)

table S6. CTC counts per milliliter as reported by notable CTC enrichment methods (non–culture-based).

Principle	Name	Average CTC counts per ml blood	Specificity	Sensitivity	Ref.
Antigen recognition	CellSearch	0-8 (Median: 0)	High	Low	(*2*)
	HB-chip	12 - 3,167 (Median: 63)	Low	Higher	(*3*)
Size-based sorting	High-definition (HD)-CTC device	5-199 (Median: 49.3)	Low	Higher	(*4*)
	Spiral inertial microfluidics	12-1,275 (Median: 55)			(*5*)

Other Supplementary Files

(Please refer to data file Movie S1)

movie S1. Illustration of seeding, growth, and drug flow.